

Experimental observation of interlayer perpendicular standing spin wave mode with low damping in skyrmion-hosting $[Pt/Co/Ta]_{10}$ multilayer

Zhen-Dong Chen(陈振东), Mei-Yang Ma(马眉扬), Sen-Fu Zhang(张森富), Mang-Yuan Ma(马莽原), Zi-Zhao Pan(潘咨兆), Xi-Xiang Zhang(张西祥), Xue-Zhong Ruan(阮学忠), Yong-Bing Xu(徐永兵), and Fu-Sheng Ma(马付胜)

Citation: Chin. Phys. B, 2022, 31 (**11**): 117501. DOI: 10.1088/1674-1056/ac7bf9

What follows is a list of articles you may be interested in

Angle-dependent spin wave spectra of permalloy ring arrays

Shuxuan Wu(吴书旋), Zengtai Zhu(朱增泰), Yunxu Ma(马云旭), Jinwu Wei(魏晋武), Senfu Zhang(张森富), Jianbo Wang(王建波), and Qingfang Liu(刘青芳)

Chin. Phys. B, 2022, 31 (**11**): 117505. DOI: 10.1088/1674-1056/ac8af9

Interaction region of magnon-mediated spin torques and novel magnetic states

Zai-Dong Li(李再东), Qi-Qi Guo(郭奇奇), Yong Guo(郭永), Peng-Bin He(贺鹏斌), and Wu-Ming Liu(刘伍明)

Chin. Phys. B, 2021, 30 (**10**): 107506. DOI: 10.1088/1674-1056/ac04a8

Spin waves and transverse domain walls driven by spin waves: Role of damping

Zi-Xiang Zhao(赵梓翔), Peng-Bin He(贺鹏斌), Meng-Qiu Cai(蔡孟秋), Zai-Dong Li(李再东)

Chin. Phys. B, 2020, 29 (**7**): 077502. DOI: 10.1088/1674-1056/ab90e5

Voltage control of ferromagnetic resonance and spin waves

Xinger Zhao(赵星儿), Zhongqiang Hu(胡忠强), Qu Yang(杨曲), Bin Peng(彭斌), Ziyao Zhou(周子尧), Ming Liu(刘明)

Chin. Phys. B, 2018, 27 (**9**): 097505. DOI: 10.1088/1674-1056/27/9/097505

Angle-dependent spin waves in antidot bilayers

Hu Chun-Lian (胡春莲), Liao Leng (廖棱), Stamps R

Chin. Phys. B, 2014, 23 (**12**): 127501. DOI: 10.1088/1674-1056/23/12/127501

Experimental observation of interlayer perpendicular standing spin wave mode with low damping in skyrmion-hosting $[Pt/Co/Ta]_{10}$ multilayer

Zhen-Dong Chen(陈振东)[1,†], Mei-Yang Ma(马眉扬)[2,†], Sen-Fu Zhang(张森富)[3,4], Mang-Yuan Ma(马莽原)[1], Zi-Zhao Pan(潘咨兆)[1], Xi-Xiang Zhang(张西祥)[4], Xue-Zhong Ruan(阮学忠)[2,‡], Yong-Bing Xu(徐永兵)[2,§], and Fu-Sheng Ma(马付胜)[1,¶]

[1] *Jiangsu Key Laboratory of Opto-Electronic Technology, Center for Quantum Transport and Thermal Energy Science, School of Physics and Technology, Nanjing Normal University, Nanjing* 210046, *China*

[2] *Jiangsu Provincial Key Laboratory of Advanced Photonic and Electronic Materials, School of Electronic Science and Engineering, Nanjing University, Nanjing* 210093, *China*

[3] *School of Physical Science and Technology, Lanzhou University, Lanzhou* 730000, *China*

[4] *Physical Science and Engineering Division (PSE), King Abdullah University of Science and Technology (KAUST), Thuwal* 23955-6900, *Saudi Arabia*

(Received 12 May 2022; revised manuscript received 21 June 2022; accepted manuscript online 27 June 2022)

An interlayer perpendicular standing spin wave mode is observed in the skyrmion-hosting $[Pt/Co/Ta]_{10}$ multilayer by measuring the time-resolved magneto-optical Kerr effect. The observed interlayer mode depends on the interlayer spin-pumping and spin transfer torque among the neighboring Co layers. This mode shows monotonically increasing frequency-field dependence which is similar to the ferromagnetic resonance mode, but within higher frequency range. Besides, the damping of the interlayer mode is found to be a relatively low constant value of 0.027 which is independent of the external field. This work expounds the potential application of the $[heavy\text{-}metal/ferromagnetic\text{-}metal]_n$ multilayers to skyrmion-based magnonic devices which can provide multiple magnon modes, relatively low damping, and skyrmion states, simultaneously.

Keywords: dynamic properties of magnetization, spin waves, domain structure, magnetic properties of interfaces

PACS: 75.40.Gb, 75.30.Ds, 75.70.Kw, 75.70.Cn **DOI:** 10.1088/1674-1056/ac7bf9

1. Introduction

With the development of conventional complementary metal–oxide–semiconductor (CMOS) devices approaching to the limit of the Moore's law, people have paid much attention to beyond-CMOS devices which use other degrees of freedom to code information instead of electron charge.[1–5] Since the 1990s, magnonics has been identified to be particularly promising in all approaches to developing beyond-CMOS devices.[6–14] Magnonics is a new research field which focuses on the characteristics of spin waves, and they are used to carry and process information.[8,10,11] Magnonic devices are expected to possess significant advantages such as high speed, low energy dissipation, broad frequency ranges from gigahertz to terahertz, *et al.*[10,11] Because of such advantages, lots of magnonic devices have been designed, such as magnon based nano-oscillators, interferometers, logic gates, and transistors.[10,11,13,15–20]

Further studies of magnonics and magnonic devices require a platform to be able to excite different spin wave modes. Thus, the concept of magnonic crystals (MCs) was put forward, in which spin waves can be modulated into magnon bands via artificial periodical structures of magnetic properties.[10,12,21–25] Among new magnetic media, skyrmion-based MCs (SMCs) have attracted much attention in which the periodical structures are constituted by skyrmions.[12,26–31] The SMCs show great potential applications in dynamic and functional magnonic devices due to their dynamical tunability.[26,28] And in recent years, the topological nontrivial magnon bands and the chiral edge magnon states were predicted to exist in SMCs, which provides a new kind of platform for topological physics study and application of the chiral edge magnon states with low energy dissipation.[29–31] In experimental studies, there are a variety of artificial thin-film skyrmion systems with interfacial Dzyaloshinskii–Moriya interactions (iDMI) which can be the candidates for building SMCs, such as Pt/CoFeB/MgO, Pt/Co/Ta, Ir/Fe/Co/Pt, *etc.*[32–37] Additionally, the artificial systems with iDMI can be providers of chiral spin waves, and show a potential application in functional chiral magnonics.[38–40] However, there are rare experimental researches of the dynamic properties

[†]These authors contributed equally to this work.
[‡]Corresponding author. E-mail: xzruan@nju.edu.cn
[§]Corresponding author. E-mail: ybxu@nju.edu.cn
[¶]Corresponding author. E-mail: phymafs@njnu.edu.cn

© 2022 Chinese Physical Society and IOP Publishing Ltd

of these skyrmion-hosting thin-film systems, and the SMCs based on these platforms remains unrealized. The most significant factor to limit the study of their dynamic properties and their applications in SMCs is the large damping value which is mostly above 0.1.[41,42] In recent years, the skyrmion-hosting thin-films in the form of [heavy-metal (HM)/ferromagnetic-metal (FM)/heavy-metal (HM)]$_n$ multilayers are reported to show relatively low damping of less than 0.05.[37,43] These findings provide a promising platform for studying the dynamic spin wave modes of the skyrmion-hosting thin-film systems, and promotes the experimental realization of SMCs.

In this work, we experimentally study the dynamic properties of the skyrmion-hosting [Pt/Co/Ta]$_{10}$ multilayer by measuring the time-resolved magneto-optical Kerr effect (TR-MOKE). An interlayer perpendicular standing spin wave (PSSW) mode in the multilayers is observed. We declare that this interlayer PSSW mode depends on the spin pumping and spin transfer torque among the neighboring Co layers. Furthermore, by comparing the effective damping of the interlayer PSSW mode and the ferromagnetic resonance (FMR) mode, we find that the damping of the interlayer PSSW mode keeps a relatively low constant value of 0.027 and is independent of the external magnetic field. Our results point out prospect of obtaining multiple and tunable spin wave modes with specific frequency and relatively low damping in skyrmion-hosting [HM/FM/HM]$_n$ multilayer structures, thus can make the multilayers a potential platform for SMCs.

2. Experiments

The multilayer stack, Ta(3 nm)/[Pt(1.5 nm)/Co(2.1 nm)/Ta(1 nm)]$_{10}$, is deposited on thermally oxidized Si substrate by DC magnetron sputtering at room temperature. The pressure of the Ar gas is 0.4 Pa. The base pressure is lower than $\sim 2\times10^{-5}$ Pa. The in-plane and out-of-plane hysteresis loops of the multilayer film are measured at room temperature by vibrating sample magnetometry (VSM). And the anomalous Hall resistance is measured by a custom-built system for magnetoelectronic transport measurements at room temperature. In order to directly clarify the existence of the skyrmion state, the multilayer film is also deposited on the Si_3N_4 membrane by the same method and structure. The Lorentz transmission electron microscopy (L-TEM) imaging is carried out by using an FEI Titan Cs image TEM in Lorentz mode (the Fresnel imaging mode) at 300 kV, and the out-of-plane field is set to be at a tilt angle of $\theta = 30^\circ$ with respect to the normal direction of the film.[36,44] The dynamic characteristics of the multilayer stack are investigated via polar TR-MOKE measurements at room temperature. The sketch of the multilayer stack and the geometric configuration of the TR-MOKE measurements are shown in Fig. 1(a). During the TR-MOKE measurements, the pump laser is vertically injected on the surface of the film, and the probe laser is nearly vertically injected at a small angle deviated from the normal direction. The wavelength, spot diameter focused onto the film surface, and the fluence of the pump (probe) laser are 800 nm (400 nm), 300 μm (180 μm), and 3.10 mJ/cm^2 (20.54 μJ/cm^2), respectively. The pulse duration of the pump laser and the probe laser are both $\sim$ 50 fs. The external magnetic fields are set to be in the x–z plane with the azimuth angle $\theta = 60^\circ$, 70°, 80°, and their magnitudes change from 429.4 mT to 992.0 mT.

3. Results

In order to obtain the saturation field and magnetization processes of the multilayer stack, VSM measurements are executed with the field along out-of-plane ($\theta = 0^\circ$) and in-plane ($\theta = 90^\circ$) direction as shown in Fig. 1(b). It obviously exhibits that the saturation fields are both $\sim$ 300 mT for the above two cases. The similar saturation fields along the in-plane direction and the out-of-plane direction imply the presence of a perpendicular magnetic anisotropy which has a magnitude similar to the demagnetization energy in the Co layer of the stack.[45] The saturated magnetization (M_s) of the Co layer is also obtained to be $\sim$ 378 kA/m (378 emu/cm^3). This magnetization value is comparable to the values of Pt/Co/Ta multilayers in previous researches, but much lower than those of Co monolayers.[46,47] The low magnetization of the [Pt/Co/Ta]$_{10}$ multilayer stack is attributed to the intermixing at the interface of the Co layers and the Ta(Pt) layers. Furthermore, the minor loops can be found while $\mu_0 H$ is around 180 mT and -180 mT, whose irreversible characters can be attributed to the skyrmion texture.[36,44] The inset of Fig. 1(b) shows a zoom-in view of the minor loop with $\mu_0 H$ around 180 mT, serving as an example.

For confirming the existence of the skyrmion state, we analyze the topological Hall effect by comparing the anomalous Hall effect with the M–H curves.[48] Figure 1(c) shows the normalized anomalous Hall resistance ratio ($\rho_H^{meas}/\rho_H^{sat}$, where ρ_H^{meas} and ρ_H^{sat} are the measured anomalous Hall resistance ratio and the saturated anomalous Hall resistance ratio, respectively) and the M–H curve while $\mu_0 H$ is scanned from 400 mT to -400 mT. The slight difference between the two curves implies the existence of the topological Hall effect. We define the normalized anomalous Hall resistance ratio as $\rho_H^T/\rho_H^{sat} = (\rho_H^{theo} - \rho_H^{meas})/\rho_H^{sat}$, where ρ_H^T is the topological Hall resistance ratio, and ρ_H^{theo} is the theoretical anomalous Hall resistance ratio which is proportional to the magnetization M. Figure 1(d) shows the field dependence of ρ_H^T/ρ_H^{sat} while $\mu_0 H$ sweeps from 400 mT to -400 mT. It can be found that there are two peaks in the ρ_H^T/ρ_H^{sat}–H curve while $\mu_0 H$ is around 180 mT and -180 mT. The two peaks are features

of the skyrmion state, which means that the skyrmions should exist in the same H ranges as the peaks.[48]

To directly observe the domain structures of the multilayer, the L-TEM measurements are executed for the same multilayer stack deposited on the Si_3N_4 membrane with $\theta = 30°$. Figures 1(e) and 1(f) show the L-TEM image at $\mu_0 H = 0$ mT and the L-TEM image at $\mu_0 H = 170$ mT, respectively. It is exhibited obviously that when $\mu_0 H = 0$ mT, the multilayer stack shows a stripe domain state; when $\mu_0 H = 170$ mT, the disk patterns with dark–bright contrast demonstrate the presence of Néel-type skyrmions.[44] The existence of the stripe domain state and the Néel-type skyrmion state observed by L-TEM conform to the suggestion of the out-of-plane magnetization hysteresis loop and the topological Hall effect, and are also in agreement with previous observations on the L-TEM image of $[Pt/Co/Ta]_n$ multilayer stacks.[36,44]

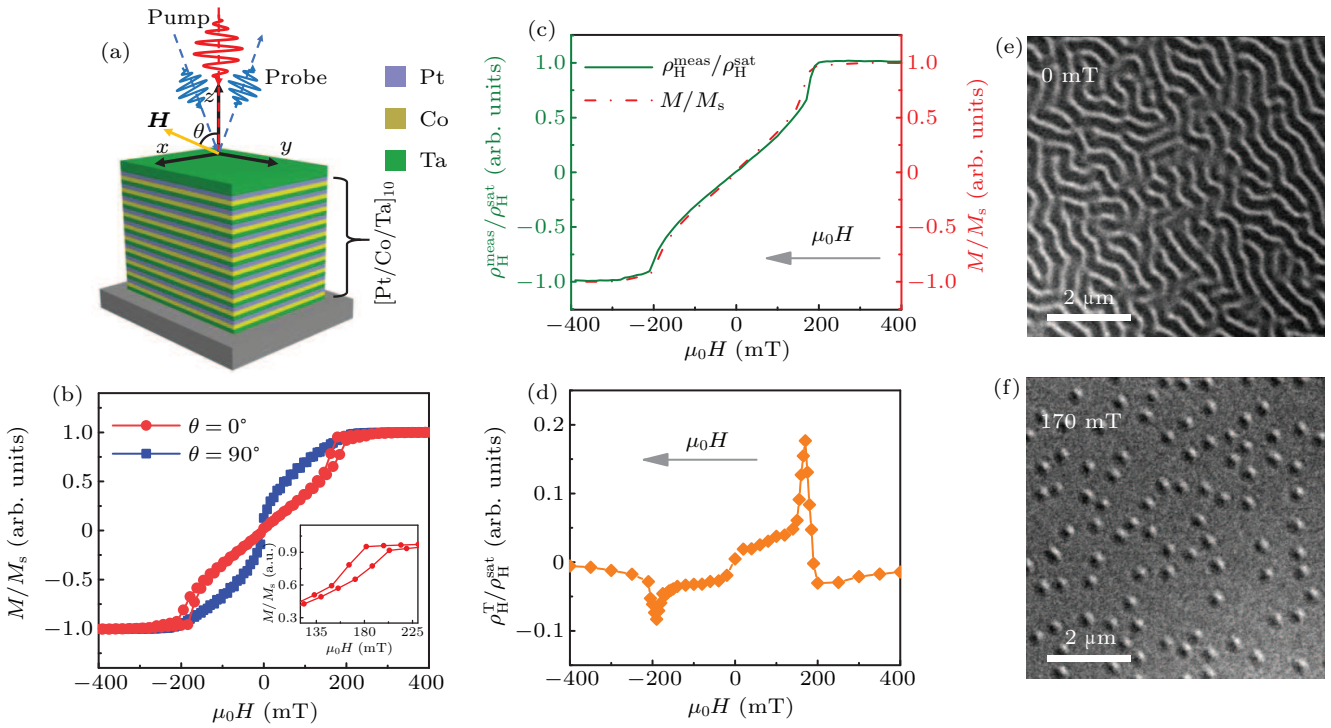


Fig. 1. (a) Illustration of Ta/$[Pt/Co/Ta]_{10}$ multilayer stack, and geometric configuration of TR-MOKE measurements, where external field $\boldsymbol{H}$ (yellow arrow) is set to be in x–z plane, θ is angle between $\boldsymbol{H}$ and z axis. Red wavy line and blue wavy lines represent pump laser and probe laser, respectively. (b) Magnetization hysteresis loop of multilayer with $\theta = 0°$ and 90°, with inset showing zoom-in view of loop with $\theta = 0°$ and $\mu_0 H$ around 180 mT. (c) ρ_H^T/ρ_H^{sat} and M–H curve with $\mu_0 H$ scanning from 400 mT to −400 mT. (d) ρ_H^T/ρ_H^{sat} curve with H scanning from 400 mT to −400 mT. L-TEM images with a tilt angel $\theta = 30°$, $\mu_0 H = 0$ mT (e) and 170 mT (f), respectively. The unit "a.u." in the inset of Fig. 1(b) is short for arb. units.

In order to investigate the dynamic processes of the stack, TR-MOKE measurements are performed under the externally applied fields at $\theta = 60°$, 70°, and 80°; as well as the magnitudes of $\mu_0 H$ changing from 429.4 mT to 992.0 mT. It should be noticed that the TR-MOKE measurements are performed under the condition of saturated magnetization with the external fields larger than 300 mT. Figure 2(a) shows a representative result of the TR-MOKE measurements with $H = 752.3$ mT and $\theta = 80°$. The obvious nodes and antinodes of the damped oscillation curve demonstrate that there are multiple dynamic modes in the multilayer stack which are excited simultaneously by the pump laser. The frequency spectrum obtained from the fast Fourier transform (FFT) result of this curve [Fig. 2(b)] shows that there are two precession modes in the multilayer stack with frequencies of 24.48 GHz and 30.15 GHz, respectively. Figures 3(a)–3(c) show the TR-MOKE curves with each θ under different external fields and Figs. 3(d)–3(f) display the corresponding frequency spectra obtained from the FFT results. Like Figs. 2(a) and 2(b), it can also be identified in Figs. 3 that there are two dynamic modes under each external field with $\theta = 60°$, 70°, and 80°. From the frequency spectra, it can also be found that for each θ, the frequency–field (f–H) dependence of both the two dynamic modes show similar monotonically increasing trends, which conform to the Kittel model.[49]

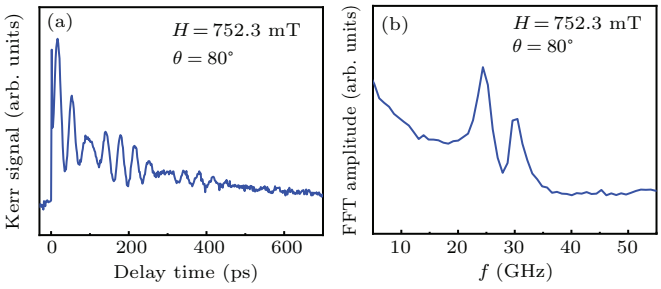


Fig. 2. (a) TR-MOKE curve with $H = 7.523$ kOe (1 Oe = 79.5775 A·m^{-1}) and $\theta = 80°$, and (b) corresponding frequency spectrum obtained from FFT result, respectively.

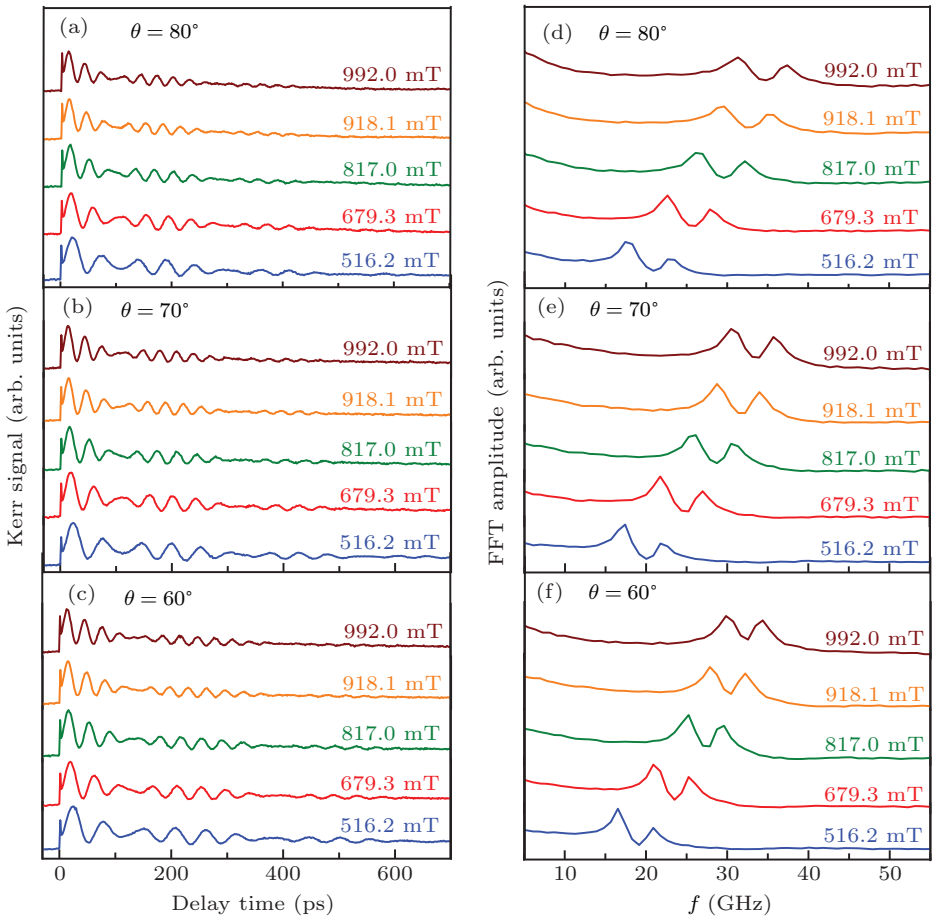


Fig. 3. TR-MOKE curves with different external fields with $\theta = 80°$ (a), 70° (b), and 60° (c), as well as the frequency spectra obtained from the corresponding FFT results with $\theta = 80°$ (d), 70° (e), and 60° (f).

4. Discussion

Since the $[Pt/Co/Ta]_{10}$ multilayer stack is an in-plane uniform medium, and the probe laser spot focused on the multilayer is overlapped with the pump laser spot with smaller diameter, the probe laser cannot detect multiple in-plane spin wave modes in the multilayer.[50–52] Considering the similar monotonically increasing f–H relations, the two dynamic modes can be recognized as the FMR mode and the PSSW mode.[49,53,54] However, the PSSW mode in the single Co layer cannot arise in the measurements due to its high frequency which should be hundreds of gigahertz or near terahertz. This high frequency is induced by the ultrathin film with a thickness of 2.1 nm and the strong Heisenberg exchange coupling.[55,56] Thus, it can be expected that the multilayer structures can provide interlayer PSSW modes depending on interlayer coupling. In previous researches, researchers have investigated several interlayer couplings which have an effect on spin wave propagation in a multilayer structure, such as dipolar coupling,[57–60] interlayer exchange coupling,[56,61,62] Ruderman–Kittel–Kasuya–Yosida (RKKY) coupling,[63,64] spin pumping, and spin transfer torque.[65] However, the first three factors can be excluded from the $[Pt/Co/Ta]_{10}$ multilayer stack: the interlayer spin waves propagating via interlayer dipolar coupling are demonstrated to be degenerated with the FMR mode;[57] the interlayer exchange coupling and the RKKY coupling among the Co layers can be blocked by the Pt and Ta layers which possess a total thickness of 2.5 nm. Thus, we declare that the two dynamic modes excited in the $[Pt/Co/Ta]_{10}$ stack are the FMR mode and the interlayer PSSW mode, which depend on spin pumping and spin transfer torque, respectively.[65] Figures 4(a) and 4(b) illustrate the moment precession of the FMR mode and the interlayer PSSW mode, as well as the effect of the spin pumping and spin transfer torque. While the moments of a single Co layer are precessing, the layer will inject two spin currents into neighboring nonmagnetic metal layers. The two spin currents are attributed to spin pumping effect and spin accumulation effect, respectively. And they will propagate through the nonmagnetic metal layer, and result in a damping-like torque (τ_{SP}) and a field-like torque (τ_{ST}) at the interface between the nonmagnetic metal layer and the nearest two Co layers. Owing to the torques, spin waves can propagate through different Co layers, resulting in the generation of interlayer PSSW modes in the $[Pt/Co/Ta]_{10}$ multilayers. The f–H dependence of the interlayer PSSWs in such ferromagnetic/nonmagnetic multilayers can be written as follows:[65]

$$f = \frac{\mu_0\gamma}{2\pi}\sqrt{\left[H + \frac{2A_{\rm ex}}{\mu_0 M_{\rm s}}k^2 - \left(M_{\rm s} - \frac{2K_\perp}{\mu_0 M_{\rm s}}\right)\cos 2\theta\right]\left(H + \frac{2A_{\rm ex}}{\mu_0 M_{\rm s}}k^2\right)}, \tag{1}$$

where f is the frequency of the spin wave, γ is the gyromagnetic ratio, H is the magnitude of the external fields, $M_{\rm s}$ is the saturation magnetization of the Co layers, $A_{\rm ex}$ is the exchange coupling constant, $K_\perp$ is the perpendicular magnetic anisotropy constant, and k is the wave vector of the PSSWs. When $k = 0$, equation (1) will reduce to the FMR form; and when $k \neq 0$, equation (1) can describe the characteristics of PSSWs. For PSSWs in single ferromagnetic films, $k = 2\pi/\lambda = p\pi/d$ where λ is the wavelength of the PSSW, p is an integer number, and d is the thickness of the ferromagnetic films. Owing to the positive value of $A_{\rm ex}$ in Co layers, it can be noticed that under the same external field H, the frequency of perpendicular spin waves is higher than that of the FMR mode. Thus, the two dynamic modes observed in the $[Pt/Co/Ta]_{10}$ multilayer stack can be identified to be that the low frequency mode is FMR mode and the high frequency mode is PSSW mode. The experimentally observed f–H relations with $\theta = 60°$, 70°, and 80° are shown in Figs. 4(c)–4(e).

By fitting the f–H relations of the FMR mode and the PSSW mode via Eq. (1) with $k = 0$ and $k \neq 0$ respectively, it can be obtained that $\gamma/2\pi = 28.3$ GHz/T, $K_\perp = 3.68 \times 10^4$ J/m^3, and $2A_{\rm ex}k^2/\mu_0 M_{\rm s} = 143$ mT. While we set $A_{\rm ex} = 10$ pJ/m,[66,67] then we can obtain the wavelength $\lambda = 2\pi/k = 130$ nm; while we set $A_{\rm ex} = 5$ pJ/m, we can obtain $\lambda = 82$ nm. These λ values are much larger than the thickness of the single Co layer (2.1 nm), and are comparable to the doubled total thickness of the $[Pt/Co/Ta]_{10}$ multilayer stack, which also confirms that the high-frequency mode is the interlayer PSSW mode. In the above analysis, the effect of iDMI is not taken into account. Since it has been demonstrated that if the in-plane wave vector of the spin wave is zero, the iDMI will not affect the characteristics of the spin waves.[40,47,68,69]

Furthermore, we compare the effective damping of the FMR mode and the interlayer PSSW mode. The effective damping can be obtained by the following equations:[70,71]

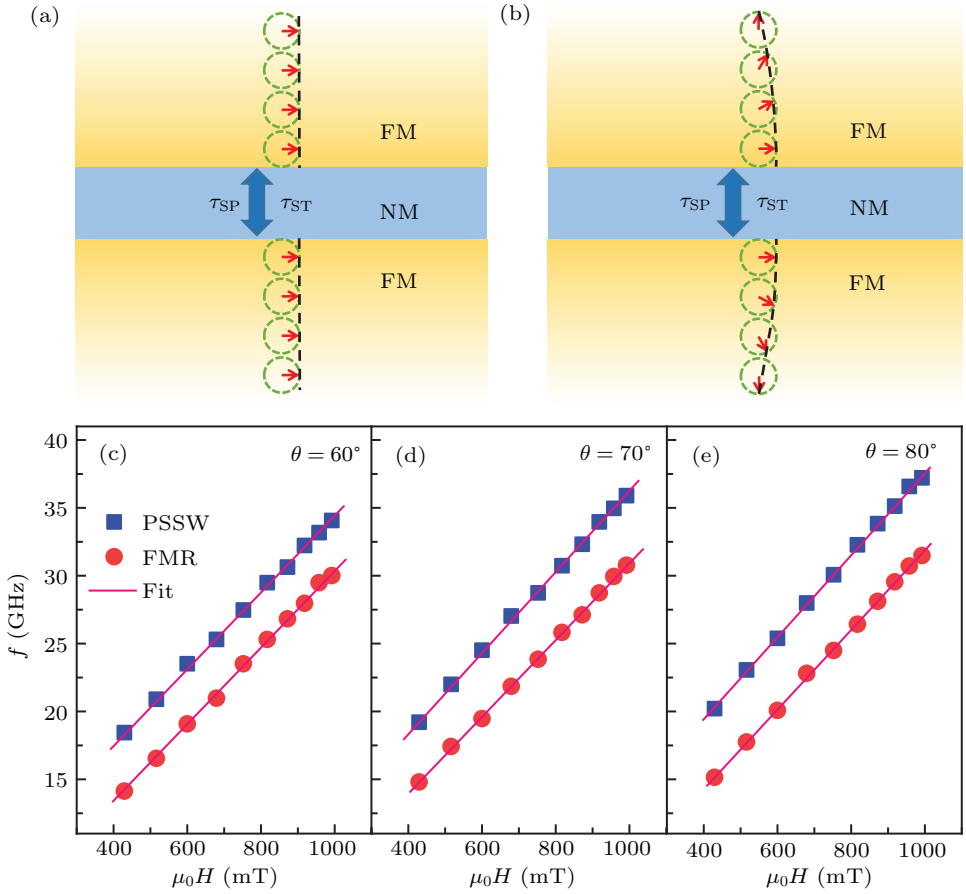


Fig. 4. Illustrations of the moment precession for (a) FMR mode and (b) interlayer PSSW mode in multilayers, respectively, with blue arrows with double ends representing effect of spin pumping and spin transfer torque, and for [(c)–(e)] f–H dependence of FMR mode and PSSW mode with $\theta = 60°$, 70°, and 80°, with pink lines denoting fitting results with Eq. (1).

$$\alpha_{\mathrm{FMR}} = \frac{1}{2\pi f_{\mathrm{FMR}} \tau_{\mathrm{FMR}}}, \tag{2a}$$

$$\alpha_{\mathrm{PSSW}} = \frac{1}{2\pi f_{\mathrm{PSSW}} \tau_{\mathrm{PSSW}}}, \tag{2b}$$

where α_{FMR} (α_{PSSW}), f_{FMR} (f_{PSSW}), and τ_{FMR} (τ_{PSSW}) are the effective damping, frequency, relaxation time of the FMR (interlayer PSSW) mode, respectively. The relaxation time τ_{FMR} and τ_{PSSW} can be obtained by fitting the TR-MOKE data via the equation:

$$\begin{aligned}\theta_{\mathrm{Kerr}} = {} & A_{\mathrm{FMR}} \mathrm{e}^{-\frac{t}{\tau_{\mathrm{FMR}}}} \sin\left(2\pi f_{\mathrm{FMR}} t + \varphi_{\mathrm{FMR}}\right) \\ & + A_{\mathrm{PSSW}} \mathrm{e}^{-\frac{t}{\tau_{\mathrm{PSSW}}}} \sin\left(2\pi f_{\mathrm{PSSW}} t + \varphi_{\mathrm{PSSW}}\right) \\ & + A_1 \mathrm{e}^{-t/\tau_0}, \end{aligned} \tag{3}$$

where θ_{Kerr} is the Kerr rotation, A_{FMR} (A_{PSSW}) and φ_{FMR} (φ_{PSSW}) are the amplitude and phase of the FMR (interlayer PSSW) mode, respectively, and $A_1 \mathrm{e}^{-t/\tau_0}$ is the exponential decay background. The first term on the right-hand side of Eq. (3) corresponds to the precession of the FMR mode, and the second term corresponds to the interlayer PSSW mode. Figures 5(a)–5(c) show the curves of effective damping versus external field with $\theta = 60°$, 70°, and 80°. It can be clearly seen that α_{FMR} reduces and approaches to 0.03 with external field increasing. It is a normal rule for α_{FMR} because α_{FMR} is mainly determined by the extrinsic factors such as the inhomogeneous magnetization which is attributed to the inhomogeneous magnetic anisotropic field. The increasing H will suppress the contribution of the inhomogeneous magnetization, and makes α_{FMR} approach to the intrinsic Gilbert damping value.[70,71] However, it can be found that α_{PSSW} always maintains a relatively low value around 0.027 which is independent of the magnitudes and the directions of the external fields. The stable α_{PSSW} with a relatively low value can be attributed to the weak inhomogeneity of the exchange field. Unlike α_{FMR}, the α_{PSSW} is mainly determined by the inhomogeneity of the exchange field which is generally weaker than the inhomogeneity of the magnetic anisotropic field. Thus, the α_{PSSW} is lower than α_{FMR} and closer to the intrinsic value of the Gilbert damping of the magnetic films.[72] And more importantly, it suggests that the $[\mathrm{Pt/Co/Ta}]_{10}$ multilayer stack possesses a relatively low intrinsic damping, which is much lower than the intrinsic damping of most of skyrmion-hosting thin-film systems (mostly above 0.1).[38,39] This low damping means that the $[\mathrm{Pt/Co/Ta}]_{10}$ multilayers are also the potential platforms for studying the dynamic properties of the thin-film skyrmion systems and experimentally realizing SMCs.

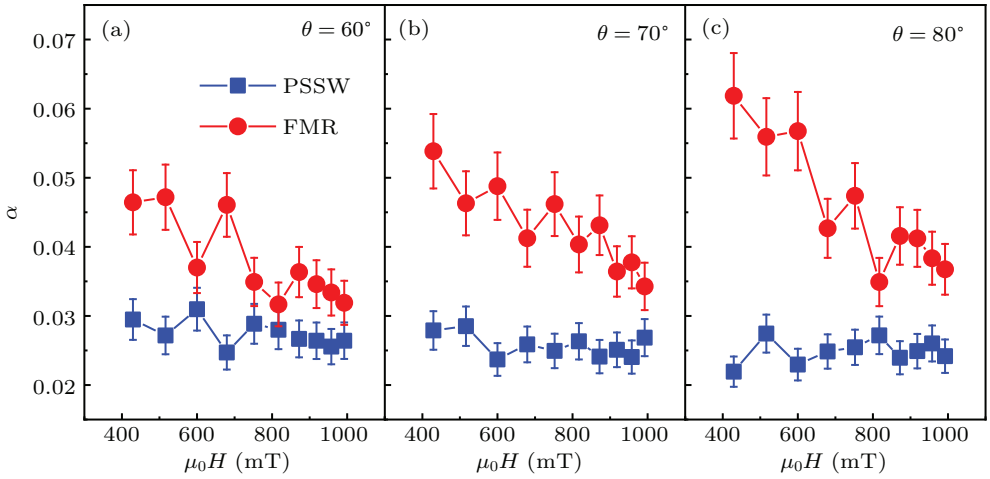


Fig. 5. Effective damping of the FMR mode and the PSSW mode with $\theta = 60°$ (a), 70° (b), and 80° (c).

5. Conclusions

In this work, we have experimentally studied the dynamic properties of the skyrmion-hosting $[\mathrm{Pt/Co/Ta}]_{10}$ multilayers by TR-MOKE measurements. An interlayer PSSW mode is observed. This interlayer dynamic mode is attributed to the spin pumping and spin transfer torque, and shows similar monotonically-increasing f–H relationships to that from the FMR mode. Furthermore, the damping of the interlayer PSSW mode is observed to be independent of the magnitudes and the directions of the external fields, and show a relatively low valuecompared with that of FMR mode. Our findings provide a new approach to obtaining the multiple and tunable spin wave modes, relatively low damping, and skyrmion states via building $[\mathrm{HM/FM/HM}]_n$ multilayer structures with iDMI, thus can expand the scope of applications of the $[\mathrm{HM/FM/HM}]_n$ multilayers as potential platforms for the experimental realization of SMCs.

Acknowledgements

Project supported by the National Natural Science Foundation of China (Grant Nos. 12074189, 11704191, 11774160, and 61427812), the Natural Science Foundation of Jiangsu Province, China (Grant Nos. BK20192006 and BK20211144), and the Postdoctoral Research Funding Program of Jiangsu

Province, China (Grant No. 2021K503C).

References

[1] Hutchby J A, Bourianoff G I, Zhirnov V V and Brewer J E 2002 *IEEE Circuits Dev. Mag.* **18** 28

[2] Bernstein K, Cavin R K, Porod W, Seabaugh A and Welser J 2010 *Proc. IEEE* **98** 2169

[3] Nikonov D E and Young I A 2013 *Proc. IEEE* **101** 2498

[4] Nikonov D E and Young I A 2015 *IEEE J. Explor. Solid-State Comput. Devices Circuits* **1** 3

[5] Pan C and Naeemi A 2017 *Proc.* 2017 *Des. Autom. Test Eur. DATE* **2017** 133

[6] Vasseur J O, Dobrzynski L, Djafari-Rouhani B and Puszkarski H 1996 *Phys. Rev. B* **54** 1043

[7] Neusser S and Grundler D 2009 *Adv. Mater.* **21** 2927

[8] Kruglyak V V, Demokritov S O and Grundler D 2010 *J. Phys. D: Appl. Phys.* **43** 264001

[9] Nikitov S A, Kalyabin D V, Lisenkov I V, *et al.* 2015 *Physics-Uspekhi* **58** 1002

[10] Chumak A V, Vasyuchka V I, Serga A A and Hillebrands B 2015 *Nat. Phys.* **11** 453

[11] Mahmoud A, Ciubotaru F, Vanderveken F, Chumak A V, Hamdioui S, Adelmann C and Cotofana S 2020 *J. Appl. Phys.* **128** 161101

[12] Yu H, Xiao J and Schultheiss H 2021 *Phys. Rep.* **905** 1

[13] Zhang Z, Jin L, Wen T, Liao Y, Tang X, Zhang H and Zhong Z 2020 *Sci. Sin. Informationis* **50** 67

[14] Barman A, Gubbiotti G, Ladak S, *et al.* 2021 *J. Phys.: Condens. Matter* **33** 413001

[15] Demidov V E, Urazhdin S, Ulrichs H, Tiberkevich V, Slavin A, Baither D, Schmitz G and Demokritov S O 2012 *Nat. Mater.* **11** 1028

[16] Schneider T, Serga A A, Leven B, Hillebrands B, Stamps R L and Kostylev M P 2008 *Appl. Phys. Lett.* **92** 022505

[17] Lee K S and Kim S K 2008 *J. Appl. Phys.* **104** 053909

[18] Chumak A V, Serga A A and Hillebrands B 2014 *Nat. Commun.* **5** 4700

[19] Klingler S, Pirro P, Brächer T, Leven B, Hillebrands B and Chumak A V 2014 *Appl. Phys. Lett.* **105** 152410

[20] Yu W, Lan J and Xiao J 2020 *Phys. Rev. Appl.* **13** 024055

[21] Nikitov S A, Tailhades P and Tsai C S 2001 *J. Magn. Magn. Mater.* **236** 320

[22] Puszkarski H and Krawczyk M 2003 *Solid State Phenom.* **94** 125

[23] Chumak A V, Serga A A and Hillebrands B 2017 *J. Phys. D: Appl. Phys.* **50** 244001

[24] Zakeri K 2020 *J. Phys. Condens. Matter* **32** 363001

[25] Stamps R L, Breitkreutz S, Åkerman J, Chumak A V, Otani Y, Bauer G E W, Thiele J U, Bowen M, Majetich S A, Kläui M, Prejbeanu I L, Dieny B, Dempsey N M and Hillebrands B 2014 *J. Phys. D. Appl. Phys.* **47** 333001

[26] Ma F, Zhou Y, Braun H B and Lew W S 2015 *Nano Lett.* **15** 4029

[27] Chen Z and Ma F 2021 *J. Appl. Phys.* **130** 090901

[28] Roldán-Molina A, Santander M J, Nunez A S and Fernández-Rossier J 2015 *Phys. Rev. B* **92** 245436

[29] Roldán-Molina A, Nunez A S and Fernández-Rossier J 2016 *New J. Phys.* **18** 045015

[30] Kim S K and Tserkovnyak Y 2017 *Phys. Rev. Lett.* **119** 077204

[31] Diáz S A, Hirosawa T, Klinovaja J and Loss D 2020 *Phys. Rev. Res.* **2** 013231

[32] Tokura Y and Kanazawa N 2020 *Chem. Rev.* **121** 2857

[33] Everschor-Sitte K, Masell J, Reeve R M and Kläui M 2018 *J. Appl. Phys.* **124** 240901

[34] Fert A, Reyren N and Cros V 2017 *Nat. Rev. Mater.* **2** 17031

[35] Wiesendanger R 2016 *Nat. Rev. Mater.* **1** 16044

[36] Zhang S, Zhang J, Wen Y, Chudnovsky E M and Zhang X 2018 *Appl. Phys. Lett.* **113** 192403

[37] Flacke L, Ahrens V, Mendisch S, Körber L, Böttcher T, Meidinger E, Yaqoob M, Müller M, Liensberger L, Kákay A, Becherer M, Pirro P, Althammer M, Geprägs S, Huebl H, Gross R and Weiler M 2021 *Phys. Rev. B* **104** L100417

[38] Wang H, Chen J, Liu T, Zhang J, Baumgaertl K, Guo C, Li Y, Liu C, Che P, Tu S, Liu S, Gao P, Han X, Yu D, Wu M, Grundler D and Yu H 2020 *Phys. Rev. Lett.* **124** 027203

[39] Chen J, Hu J and Yu H 2021 *ACS Nano* **15** 4372

[40] Szulc K, Mendisch S, Mruczkiewicz M, Casoli F, Becherer M and Gubbiotti G 2021 *Phys. Rev. B* **103** 134404

[41] Satywali B, Ma F, He S, Raju M, Kravchuk V P, Garst M, Soumyanarayanan A and Panagopoulos C 2018 arXiv preprint arXiv: 1802.03979

[42] Litzius K, Lemesh I, Krüger B, Bassirian P, Caretta L, Richter K, Büttner F, Sato K, Tretiakov O A, Förster J, Reeve R M, Weigand M, Bykova I, Stoll H, Schütz G, Beach G S D and Klaüi M 2016 *Nat. Phys.* **13** 170

[43] Satywali B, Kravchuk V P, Pan L, Raju M, He S, Ma F, Petrović A P, Garst M and Panagopoulos C 2021 *Nat. Commun.* **12** 1909

[44] Zhang S, Zhang J, Wen Y, Chudnovsky E M and Zhang X 2018 *Commun. Phys.* **1** 36

[45] Zhang S, Zhang J, Wen Y, Peng Y, Qiu Z, Matsumoto T and Zhang X 2020 *Appl. Phys. Lett.* **116** 142402

[46] Woo S, Mann M, Tan A J, Caretta L and Beach G S D 2014 *Appl. Phys. Lett.* **105** 212404

[47] Sud A, Tacchi S, Sagkovits D, Barton C, Sall M, Diez L H, Stylianidis E, Smith N, Wright L, Zhang S, Zhang X, Ravelosona D, Carlotti G, Kurebayashi H, Kazakova O and Cubukcu M 2021 *Sci. Rep.* **11** 23626

[48] Soumyanarayanan A, Raju M, Oyarce A L G, Tan A K C, Im M Y, Petrovic A P, Ho P, Khoo K H, Tran M, Gan C K, Ernult F and Panagopoulos C 2017 *Nat. Mater.* **16** 898

[49] Kittel C 1958 *Phys. Rev.* **110** 1295

[50] Hiebert W K, Stankiewicz A and Freeman M R 1997 *Phys. Rev. Lett.* **79** 1134

[51] Liu Z, Sydora R D and Freeman M R 2008 *Phys. Rev. B* **77** 174410

[52] Barman A and Barman S 2009 *Phys. Rev. B* **79** 144415

[53] Mecking N 2008 *A comprehensive study of the AMR-induced microwave photovoltage, photocurrent and photoresistance in Permalloy microstrips*, Verlag Dr. Hut

[54] Lu X, Atkinson L J, Kuerbanjiang B, Liu B, Li G, Wang Y, Wang J, Ruan X, Wu J, Evans R F L, Lazarov V K, Chantrell R W and Xu Y 2019 *Appl. Phys. Lett.* **114** 192406

[55] Qin H J, Tsurkan S, Ernst A and Zakeri K 2019 *Phys. Rev. Lett.* **123** 257202

[56] Klingler S, Amin V, Geprägs S, Ganzhorn K, Maier-Flaig H, Althammer M, Huebl H, Gross R, McMichael R D, Stiles M D, Goennenwein S T B and Weiler M 2018 *Phys. Rev. Lett.* **120** 127201

[57] Camley R E, Rahman T S and Mills D L 1983 *Phys. Rev. B* **41** 261

[58] Granberg P and Mika K 1983 *Phys. Rev. B* **27** 2955

[59] Camley R E and Cottam M G 1987 *Phys. Rev. B* **35** 189

[60] Li B, Yang J and Yang G 1994 *Phys. Rev. B* **50** 9906

[61] Qin H, Hämäläinen S J and Van Dijken S 2018 *Sci. Rep.* **8** 5755

[62] Baláž P and Barnaś J 2015 *Phys. Rev. B* **91** 104415

[63] Shiota Y, Taniguchi T, Ishibashi M, Moriyama T and Ono T 2020 *Phys. Rev. Lett.* **125** 017203

[64] Sud A, Zollitsch C W, Kamimaki A, Dion T, Khan S, Iihama S, Mizukami S and Kurebayashi H 2020 *Phys. Rev. B* **102** 100403

[65] Skarsvåg H, Kapelrud A and Brataas A 2014 *Phys. Rev. B* **90** 094418

[66] Moreau-Luchaire C, Moutafis C, Reyren N, Sampaio J, Vaz C A F, Van Horne N, Bouzehouane K, Garcia K, Deranlot C, Warnicke P, Wohlhüter P, George J M, Weigand M, Raabe J, Cros V and Fert A 2016 *Nat. Nanotechnol.* **11** 444

[67] Pollard S D, Garlow J A, Yu J, Wang Z, Zhu Y and Yang H 2017 *Nat. Commun.* **8** 14761

[68] Cortés-Ortuño D and Landeros P 2013 *J. Phys. Condens. Matter* **25** 156001

[69] Moon J H, Seo S M, Lee K J, Kim K W, Ryu J, Lee H W, McMichael R D and Stiles M D 2013 *Phys. Rev. B* **88** 184404

[70] Iihama S, Ma Q, Kubota T, Mizukami S, Ando Y and Miyazaki T 2012 *Appl. Phys. Express* **5** 083001

[71] Walowski J, Kaufmann M D, Lenk B, Hamann C, McCord J and Münzenberg M 2008 *J. Phys. D.: Appl. Phys.* **41** 164016

[72] Deb M, Popova E, Hehn M, Keller N, Petit-Watelot S, Bargheer M, Mangin S and Malinowski G 2019 *Phys. Rev. Appl.* **12** 044006